Comparative Ultrastructural and Stereological Analyses of Unruptured and Ruptured Saccular Intracranial Aneurysms

Korkmaz, Emine ; Kleinloog, Rachel ; Verweij, Bon H ; Allijn, Iris E ; Hekking, Liesbeth H P ; Regli, Luca ; Rinkel, Gabriel J E ; Ruigrok, Ynte M ; Andries Post, Jan

Abstract: Insight into processes leading to rupture of intracranial aneurysms (IAs) may identify biomarkers for rupture or lead to management strategies reducing the risk of rupture. We characterized and quantified (ultra)structural differences between unruptured and ruptured aneurysmal walls. Six unruptured and 6 ruptured IA fundi were resected after microsurgical clipping and analyzed by correlative light microscopy for quantitative analysis (proportion of the vessel wall area) and transmission electron microscopy for qualitative ultrastructural analysis. Quantitative analysis revealed extensive internal elastic lamina (IEL) thickening in ruptured IA (36.3% ± 15%), while thin and fragmented IEL were common in unruptured IA (5.6% ± 7.1%). Macrophages were increased in ruptured IA (28.3 ± 24%) versus unruptured IA (2.7% ± 5.5%), as were leukocytes (12.85% ± 10% vs 0%). Vasa vasorum in ruptured but not in unruptured IA contained vast numbers of inflammatory cells and extravasation of these cells into the vessel wall. In conclusion, detection of thickened IEL, leaky vasa vasorum, and heavy inflammation as seen in ruptured IA in comparison to unruptured IA may identify aneurysms at risk of rupture, and management strategies preventing development of vasa vasorum or inflammation may reduce the risk of aneurysmal rupture.

DOI: https://doi.org/10.1093/jnen/nlx075

J Neuropathol Exp Neurol
Vol. 76, No. 10, October 2017, pp. 908–916
doi: 10.1093/jnen/nlx075

ORIGINAL ARTICLE

Comparative Ultrastructural and Stereological Analyses of Unruptured and Ruptured Saccular Intracranial Aneurysms

Emine Korkmaz, MSc, Rachel Kleinloog, MD, Bon H. Verweij, MD, PhD, Iris E. Allijn, MSc, Liesbeth H.P. Hekking, PhD, Luca Regli, MD, PhD, Gabriel J.E. Rinkel, MD, PhD, Ynte M. Ruigrok, MD, PhD, and Jan Andries Post, PhD

Abstract

Insight into processes leading to rupture of intracranial aneurysms (IAs) may identify biomarkers for rupture or lead to management strategies reducing the risk of rupture. We characterized and quantified (ultra)structural differences between unruptured and ruptured aneurysmal walls. Six unruptured and 6 ruptured IA fundi were resected after microsurgical clipping and analyzed by correlative light microscopy for quantitative analysis (proportion of the vessel wall area) and transmission electron microscopy for qualitative ultrastructural analysis. Quantitative analysis revealed extensive internal elastic lamina (IEL) thickening in ruptured IA (36.3% ± 15%), while thin and fragmented IEL were common in unruptured IA (5.6% ± 7.1%). Macrophages were increased in ruptured IA (28.3 ± 24%) versus unruptured IA (2.7% ± 5.5%), as were leukocytes (12.85% ± 10% vs 0%). Vasa vasorum in ruptured but not in unruptured IA contained vast numbers of inflammatory cells and extravasation of these cells into the vessel wall. In conclusion, detection of thickened IEL, leaky vasa vasorum, and heavy inflammation as seen in ruptured IA in comparison to unruptured IA may identify aneurysms at risk of rupture, and management strategies preventing development of vasa vasorum or inflammation may reduce the risk of aneurysmal rupture.

Key Words: Aneurysmal subarachnoid hemorrhage, Intracranial aneurysms, Ultrastructural analysis.

INTRODUCTION

Unruptured intracranial aneurysms (IA) are common with a prevalence of 3% in the general population, and the large majority of these aneurysms are small (1). Rupture of intracranial aneurysms results in subarachnoid hemorrhage, which carries a poor prognosis, with 35% case fatality and 20% case morbidity rate (2). The incidence of subarachnoid hemorrhage is only 9 per 100.000 person-years (3), indicating that the majority of unruptured IA will never rupture. In case an unruptured IA is detected the risks of rupture has to be weighed against the risks of preventive IA occlusion (4, 5). Currently, size is the most important predictor for rupture, with small IA having the smallest risk of rupture (6). Further predictors are age, sex, history of hypertension or subarachnoid hemorrhage, and IA location (6). However, these factors only explain a small proportion of the risk of rupture. Insight into the processes leading to rupture of IA may identify biomarkers for rupture, or may lead to noninvasive strategies that reduce the risk of rupture. Insight into the ultrastructural differences between unruptured and ruptured IA are crucial can provide information on the processes leading to the rupture of IA.

Studies on ultrastructural variations on IA samples are scarce (7–15) and only a subset of these studies were set to compare unruptured and ruptured IA samples (7, 11–15). In ruptured IA samples, increased disruption of the endothelium (7, 12–14), presence of vasa vasorum (12) and infiltration of inflammatory cells (7, 12–14) was found by using light microscopy (LM) combined with histochemistry (11, 12, 14, 15) or electron microscopy (EM) combined with histochemistry (7, 13). Foam cells were found in both ruptured and unruptured IA (11, 15).

Because the aneurysmal wall is ultrastructurally complex and heterogeneous, it is advantage to apply correlative microscopy by first using LM to apply stereological analysis and to identify areas of interest and subsequently by using EM to obtain qualitative information at high resolution. Such correlative microscopy providing quantitative analysis and qualitative ultrastructural analysis has not been applied before to compare unruptured and ruptured IA samples. Using this stereological analysis, we compared the integrity of the endothelial cells and the internal elastic lamina, the presence and

From the Department of Biology, Biomolecular Imaging and Cell Biology, Faculty of Science, Utrecht University, Utrecht, The Netherlands (EK, IEA, LHPH, JAP); Department of Neurology and Neurosurgery, Brain Center Rudolf Magnus, University Medical Center Utrecht, Utrecht, The Netherlands (RK, BHV, LR, GJER, YMR); and Department of Neurosurgery, University Hospital Zurich, Zurich, Switzerland (LR)

Send correspondence to: Ynte M. Ruigrok, MD, PhD, Department of Neurology and Neurosurgery, Brain Center Rudolf Magnus, University Medical Center Utrecht, Heidelberglaan 100, 3508 GA Utrecht, The Netherlands; E-mail: ij.m.ruigrok@umcutrecht.nl

Rachel Kleinloog and Emine Korkmaz were supported by a "Focus en Massa" cardiovascular research grant by the University Utrecht, The Netherlands.

The authors have no duality or conflicts of interest to declare.

Supplementary Data can be found at http://www.jnen.oxfordjournals.org.

integrity of vasa vasorum, and the presence inflammatory cell infiltration and foam cells (FC) in both luminal and abluminal layers of samples of unruptured and ruptured IA to identify potential biomarkers for aneurysmal rupture.

MATERIALS AND METHODS

Aneurysmal Samples and Clinical Data

IA samples of 12 patients were obtained from patients admitted to the University Medical Center Utrecht (UMCU) who underwent clipping of a ruptured (n = 6) or unruptured (n = 6) IA. Patient and aneurysm characteristics are shown in Supplementary Data Table S1. During microsurgery, part of the IA fundus distal to the clip was resected and immediately submerged into 4% paraformaldehyde fixative (Sigma-Aldrich) in 0.1 mol/L phosphate buffer (pH 7.4) for at least 1 hour at room temperature and stored at 4 °C until further preparation. Immediate fixation of biopsy samples is crucial to prevent induction of cellular decay. This study was approved by the Medical Ethical Review Committee of the UMCU. All patients provided written informed consent.

Sample Preparation

After initial fixation, samples were washed in 0.1 mol/L sodium cacodylate buffer (pH 7.4), cut into small blocks of approximately 1 mm^3 and fixed in half strength Karnovsky fixative (16). After 2 hours fixation at room temperature, postfixation was performed in a mixture of 1% osmium tetroxide and 1.5% potassium ferrocyanide in 0.1 mol/L sodium cacodylate (pH 7.4) for 90 minutes on ice (17). Samples were then incubated for en bloc staining with 1% tannic acid for 30 minutes at room temperature, washed with aqua dest followed by en bloc staining with 1% osmium tetroxide (OsO_4) for 30 min on ice (7). Samples were dehydrated using ethanol (70%, 80%, 90%, 95%, and 100%) followed by infiltration in a series of 1,2-propylene oxide-epon mixture (1:1, 1:2, 1:3) and finally pure epon at room temperature on a rotator over-night. Samples were oriented and embedded using flat embedding moulds (Agar) and cured at 60°C for 2 days.

Light Microscopy

Thick sections (400 nm) were cut with a diamond knife (Diatome jumbo 45°, Diatome) on an ultramicrotome (Ultracut E; Leica Microsystems). Sections were stretched and heat fixed onto glass slides, stained for 4 minutes with 1:10 dilution of mixture of equal volumes of methylene blue (Merck) in 1% disodium tetraborate (Merck) and 1% Azur2 (BDH). The complete biopsy samples were imaged using a light microscope with 40× objective (Provis AX70; Olympus) equipped with a Nikon DXM1200 digital camera and Nikon ATC-1 software (Nikon Instruments Europe, Amsterdam, The Netherlands). LM panoramas were stitched using Microsoft Research Image Composite Editor; use of the 40× objective allowed analysis at relatively high magnification in the panoramas of complete sample. The LM panoramas allow the overview of the tissue integrity and, moreover, allow easy navigation to regions of interest at the transmission electron microscopy (TEM) level.

TABLE 1. Clinical and Aneurysm Characteristics of the 12 Intracranial Aneurysm Patients

	Unruptured IA (n = 6)	Ruptured IA (n = 6)
Age (mean, range)	47 years (range 22–63)	58 years (range 40–74)
Females	4	5
Multiple IA (≥2)	3	1
Previous aneurysmal SAH	3	0
IA size (largest diameter)	10.6 mm	6 mm

IA = intracranial aneurysms; SAH = subarachnoid hemorrhage.

Transmission Electron Microscopy

Thin sections (60–70 nm), obtained right after the thick sections for LM, were collected for TEM imaging. This allowed analysis of the LM region at the ultrastructural level. Thin sections were cut with a diamond knife (Diatome 45°) on an ultramicrotome (Ultracut E; Leica Microsystems) and collected on single slot copper grids. All sections were imaged at 120 kV using FEI Tecnai-12 equipped with a side-mounted Megaview II camera with AnalysisPro software (Olympus).

Qualitative Analysis

Qualitative analysis of the endothelial cell lining integrity was scored as previously described using a score between 0 and 5 with 0 representing normal endothelial cells and 5 severely damaged or lost endothelial cells (7). Finally, specific features such as smooth muscle cell appearance, presence of thrombi were studied.

Stereological Analysis

Stereological analysis according Delesse principle (18) was employed for quantification of the following IA wall constituents at LM level: (1) internal elastic lamina, (2) vasa vasorum, (3) foam cells, and (4) inflammatory cells (i.e., macrophages, granular leukocytes and plasma cells). Samples were divided into segments, which were individually analyzed (Supplementary Data Fig. S1). The area fractions (A_A), being the percentages of the components, were determined for each segment of the samples (19). Despite the heterogeneity between the segments of a given sample, the mean values of the segments per sample in both groups was assessed and compared between unruptured and ruptured IA using the unpaired *t*-test. The relative standard error < 1% for every sample indicates reliable and precise analysis (19). An example of this approach is shown in Supplementary Data Figure S1.

RESULTS

Clinical and aneurysm characteristics of the 12 IA patients are shown in Table 1. The age of the patients ranged from 22 to 74 years, with a mean age of 47 years for patients with an unruptured IA and 58 years for patients with ruptured IA. Additional details per patient are shown in Supplementary Data Table S1.

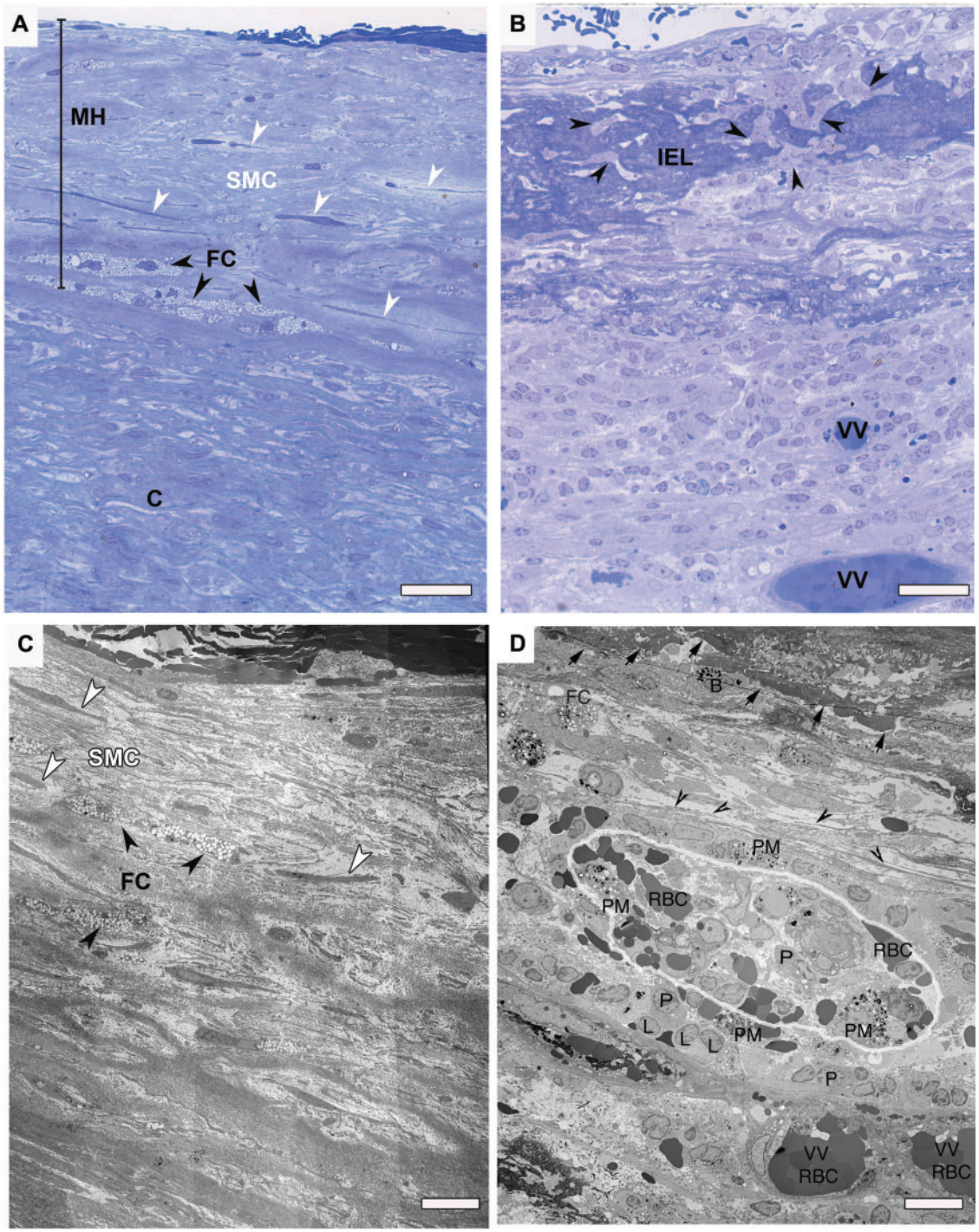

FIGURE 1. Methylene blue-Azur stained light microscopy (LM) and transmission electron microscopy (TEM) images of unruptured versus ruptured intracranial aneurysms (IA). **(A)** LM image of an unruptured aneurysm wall. Luminal layer is thickened due to myointimal hyperplasia (MH). Endothelium is missing and smooth muscle cells (SMCs) displaying "surrounding halo" (white arrowheads). Streak of foam cells (FC) could be seen in the boundary of luminal and abluminal layers (black arrowheads). Scale bar = 40 μm. **(B)** LM image of a ruptured aneurysm wall. Extensive remodeling of the wall is visible. Internal elastic lamina (IEL) is thickened with irregular margin at the luminal side. Numerous infiltrating inflammatory cells reside within IEL (arrow heads). Two vasa vasorum completely filled with red blood cells (RBCs) in the abluminal layer. Scale bar= 40 μm. **(C)** TEM micrograph of the same unruptured aneurysm wall shown in **(A)**. Extensive damage to endothelial lining is visible. Longitudinally arranged SMCs show no particular orientation to one another. Collagen, although show disarray, is present. Scale bar = 10 μm. **(D)** TEM micrograph of the same ruptured aneurysm wall shown in **(B)**. Arrows show abluminal side of the IEL.

Qualitative Analysis

Unruptured Intracranial Aneurysms.

All unruptured IA lacked an intact endothelial lining and exhibited extensive damage to the endothelium (Fig. 1A, C; Table 2). Rarely, normal appearing endothelial cells were present. In the remaining endothelial cells, we frequently observed irregular, hypertrophic endothelial cells with vesicular cytoplasms and widened intercellular gaps. Red blood cell adhesion to the IA vessel wall was detected in 4 of the 6 samples.

All of the unruptured IA samples showed thickened vascular walls due to myointimal hyperplasia (Fig. 2A). In 3 of 6 IAs, the hyperplasia was accompanied with dense or disorganized layers of smooth muscle cells (SMCs) (Fig. 1A, C). The other 3 also revealed a thickened wall; however, these only contained scattered sparse SMCs and an increased presence of collagen fibers, which constituted the predominant structure of the wall. All samples showed minimal inflammation in the luminal layer of the aneurysmal wall and when inflammatory cells were present, they consisted mainly of monocytes and macrophages (Fig. 2B–D). All unruptured vessel walls possessed disorganized wall structure without defined layers of intima, media or adventitia. In all samples, common features were heavily fragmented internal elastic lamina (IEL) remnants. In addition, some of the unruptured vessel walls showed localized areas containing FC and disorganized SMCs (Fig. 1A). In the abluminal layer, we found vasa vasorum with normal appearing endothelial cells. Within or around these vasa vasorum we observed only few inflammatory cells. This is also reflected by the quantitative data on inflammatory cells within the abluminal layer containing vasa vasorum (Table 3).

Ruptured Intracranial Aneurysms.

Correlative microscopy revealed that 4 of the 6 ruptured IA walls had complete loss of endothelial cells, the other 2 showed extensive damage to these cells. The inner (luminal) surface of the vessel wall displayed a fresh thrombus, mostly covered with amorphous fibrin and blood cells (Fig. 3A, B). Three of the 6 samples displayed organizing intraluminal thrombi, with inflammatory cells, predominantly neutrophils and macrophages, and mesenchymal like cells intermingled with collagen. In contrast to unruptured IA, we observed no hyperplasia. The structural integrity of the aneurysmal wall was heavily compromised by invasion of macrophages and leukocytes in both luminal and abluminal layers. The loss of medial SMCs, resulting in devoid areas, along with collagen disorganization or even complete loss of collagen, revealed adverse deterioration of the vessel wall. IEL was thickened significantly and infiltration of the IEL with macrophages and leukocytes was seen in 5 out of the 6 samples (Fig. 3B). Three samples showed an abundant vasa vasorum in abluminal layers (Fig. 3A, C). These vasa vasorum exhibited hypertrophic endothelial cells with cytoplasmic vacuoles. Some contained an abundance of inflammatory and occasional foam cells, indicating signs of chronic inflammation. Moreover, we observed infiltration of inflammatory cells through the vasa vasorum endothelial monolayer (Figs. 1D, 3D).

TABLE 2. Qualitative Analysis: Histological Characteristics of Endothelial Lining of Unruptured and Ruptured Saccular Intracranial Aneurysms

	Unruptured IA (n = 6)	Ruptured IA (n = 6)	*t*-test
Endothelial lining intact	0	0	
Endothelial lining damaged	5	2	
Endothelial lining totally absent	1	4	
Score of endothelial lining damage*	3.3 ± 1.03 (2–5)	4.7 ± 0.52 (4–5)	$p < 0.02$

IA = intracranial aneurysm.
*Score between 0 and 5, data represent mean ± standard deviation (range) of the score.

Heterogeneity of Pathology

Pathological alterations seen in individual unruptured and ruptured IA are heterogenic. For instance, in a ruptured sample, the percentage of IEL A_A showed variations throughout the vessel wall varying from 1.6% to 11% (Supplementary Data Fig. S1A). Similar results were obtained for the presence of FC (Supplementary Data Fig. S1B). This clearly brings forward the local nature of the events involved in IA, rather than overall modification of the vessel wall.

Quantitative (Stereological) Analysis of Unruptured and Ruptured Intracranial Aneurysm Vessel Wall Morphology

Mean percentage A_A of IEL, vasa vasorum, foam cells, macrophages, granular leukocytes and plasma cells of unruptured and ruptured IA are summarized in Table 3. The percentage of IEL A_A was 36.3%, SD 15 in ruptured IA and 5.6%, SD 7.1 in unruptured IA ($p < 0.002$). In addition, ruptured IA wall showed heavy infiltration of leukocytes and macrophages and consistent presence of antibody-producing plasma cells throughout the vessel wall, especially in the vicinity of vasa vasorum. In contrast, unruptured IA were free of leukocytes and plasma cells, however, monocytes and macrophages were present. The unruptured IA contained an almost 3 times higher foam cell A_A than ruptured IA. Vasa vasorum area fractions

FIGURE 1. Continued
Collagen is deteriorated extensively (black arrow heads). A closer look at vasa vasorum (outlined) and inflammation infiltrates. Vasa vasorum filled and surrounded with various types of granular leukocytes (L), phagocytotic macrophages (PM), plasma cells (P) and RBCs). Scale bar = 10 μm.

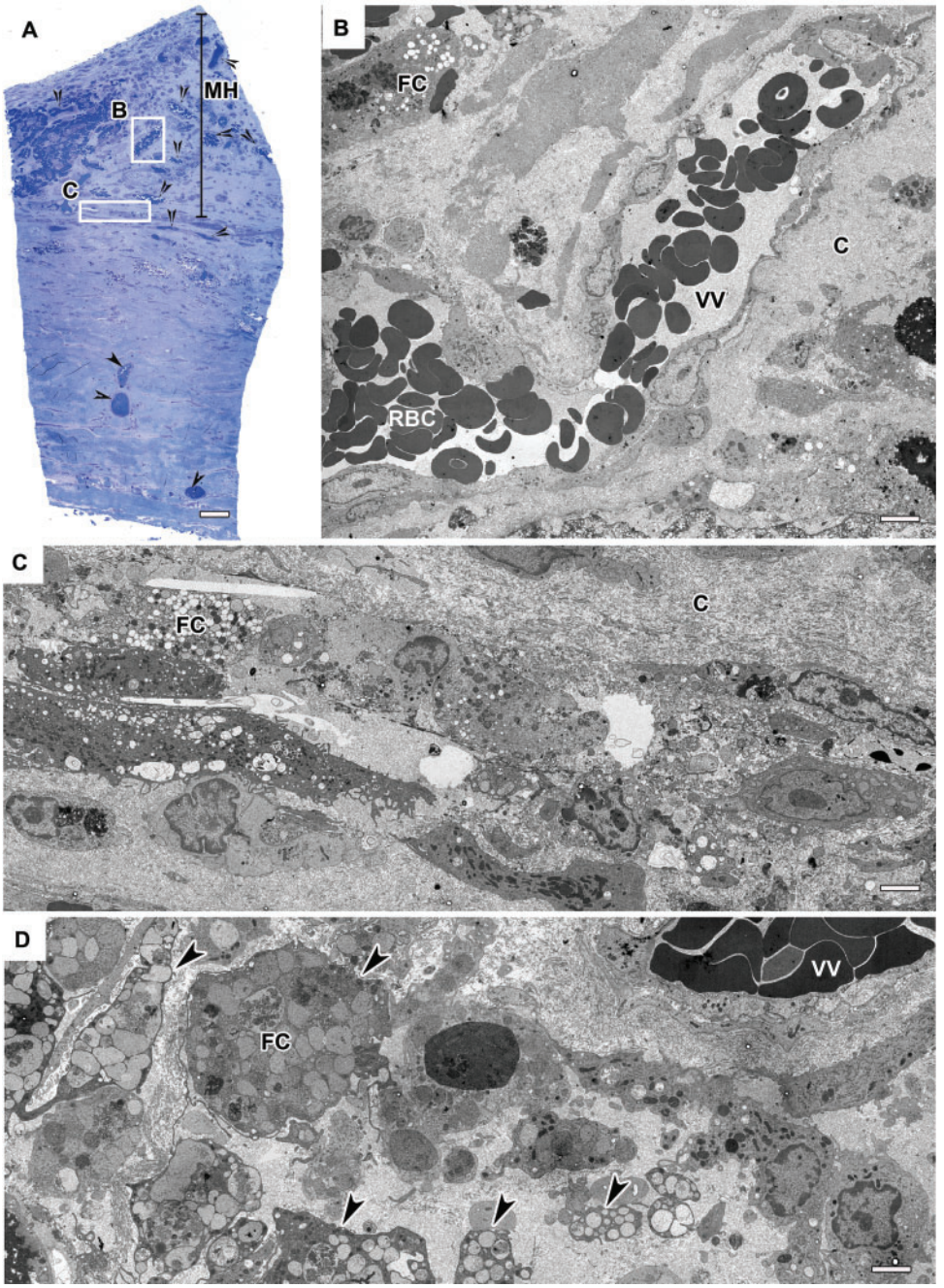

FIGURE 2. Methylene blue-Azur stained light microscopy (LM) and transmission electron microscopy (TEM) images of an unruptured intracranial aneurysm (IA). **(A)** An unruptured aneurysm wall revealing a hypocellular vascular wall with abundance of vasa vasorum complexes (arrowheads). Myointimal hyperplasia (MH) is present. Original magnification: 40×. Scale bar = 20 μm. **(B)** Large vasa vasorum filled with red blood cells (RBCs) show no sign of inflammatory cells unlike the ruptured IA. Endothelial lining show no vacuoles at tight junctions however, pseudopodia-like protrusions are present. Scale bar = 5 μm. **(C)** Foam cells (FC) and macrophages within the hypocellular wall. Disarray and abundance of collagen. Scale bar = 5 μm. **(D)** Closer look at abundance of FC and macrophages. Scale bar = 5 μm.

were comparable in both groups, mainly confined to abluminal layer and both groups harbored a case of second order vasa vasorum in luminal layer. The numerical density was higher in the unruptured IA wall, indicating that on average the size of the vasa vasorum in the ruptured IA was larger.

DISCUSSION

There are distinctive morphological characteristics between unruptured and ruptured IA, showing clear differences in their structural pathology. Qualitative and quantitative analyses revealed: (1) more extensive remodeling of the

TABLE 3. Quantitative Analysis: Histological Characteristics of Unruptured and Ruptured Aneurysmal Wall

	Unruptured IA (n = 6; mean ± SD)	Ruptured IA (n = 6; mean ± SD)	t-test
Intimal Elastic Tissue A_A	5.6% ± 7.1%	36.3% ±15%	$p < 0.01$
Foam cells A_A	5.9% ± 4.6%	2.1% ± 1.8%	NS
Vaso vasorum A_A	6.2% ± 6.6%	3.9% ± 5.8%	NS
Inflammatory Cell Infiltrations			
Macrophages A_A	2.7% ± 5.5%	28.3% ± 24%	$p < 0.03$
Plasma cells A_A	0%	0.94% ± 2.3%	NS
Granulocytes A_A	0%	12.85% ± 10%	$p = 0.01$

IA = intracranial aneurysm; SD = standard deviation; NS = not significant; *A_A = Area fraction.

aneurysmal wall in ruptured IA samples compared to unruptured samples; (2) significantly thickened IEL in ruptured IA and thin and fragmented IEL in unruptured IA; (3) extensive inflammatory cell invasion of the aneurysmal wall in the ruptured IA; (4) inflammatory cells within vasa vasorum of ruptured IA; and (5) leaky vasa vasorum in ruptured IA with extravasation of inflammatory cells into the vessel wall, showing alternate avenue of inflammatory cell invasion.

Internal Elastic Lamina

The unruptured aneurysmal wall revealed thin and fragmented IEL, while the ruptured aneurysmal wall exposed loss of structural organization, accompanied by extensive thickening and invasion of inflammatory cell infiltrates within the IEL. Fragmentation of the IEL has been observed before (7, 12–14) while 1 study also showed that such fragmentation was accompanied by the presence of mast cells (12). Structural remodeling of the IEL involves loss of the original, well organized elastin, and replacement by deposition of much less organized, patches of elastin, called intimal elastic tissue (20). The turnover of vascular elastin is very slow, with a half-life of 60–70 years, which means that structurally functional vascular elastin is primarily produced during childhood (21). Upon degradation of elastin in IA, SMCs (22) and macrophages (23) deposit intimal elastic tissue. Although this intimal elastic tissue consists of elastin, its functional properties are lost (20). Clear increase in the intimal elastic tissue deposition in the ruptured IA suggests that further structural remodeling is activated before the rupture. The thickened IEL with presence of intimal elastic tissue and inherent loss of elastic function leads to increase in wall stiffness and decreases distensibility and contributes to susceptibility to hemodynamic factors (21–24). This in combination with increased inflammation might make the lesions more prone to rupture.

Inflammation

The ruptured IA wall contained a large number of inflammatory cells, indicating pathological events in the IA wall, with detrimental contribution of ECM modulating enzymes secreted by these cells (7, 25–29). Previous studies also showed increase of inflammatory cell invasion in the ruptured IA wall including macrophages and T-lymphocytes (7, 11, 13, 14). Interestingly, lymphocytes deficient mice and mice with mutated factors of the inflammatory signaling pathway involved in macrophage infiltration suppressed IA formation, suggesting a causal role for inflammatory cells in IA (30–31). Our results are also in line with the findings of our recent whole genome gene expression study using RNA sequencing in aneurysmal tissue in which we found pathways involved in immune response enriched in ruptured as compared to unruptured IA (32). In addition, we observed small but consistent presence of antibody producing plasma cells in the ruptured, but not in the unruptured wall. In the ruptured aneurysmal wall, a gradient of plasma cells and other inflammatory cells was observed around the vasa vasorum suggesting that the cells come from the "leaky" vasa vasorum, rather than from the site of rupture. Whether the plasma cells were present before rupture or entered the wall after rupture cannot be discerned from our data. However, in our recent whole genome gene expression study immunoglobulin genes were found expressed in aneurysmal tissue (of both ruptured and unruptured IA), while they showed no expression in controls (32). Also, 1 immunoglobulin gene (*immunoglobuline kappa variable region* gene) was expressed in unruptured and not in ruptured IA (32). The expression of these immunoglobulin genes suggests the presence of plasma cells in both unruptured and ruptured IA which in turn suggests that the plasma cells as identified in our current study were already present before rupture.

Vasa Vasorum

As in 2 previous studies (8, 12) we found vasa vasorum in abluminal layers of the vessel wall of both unruptured and ruptured IA while these are not present in healthy intracranial vessel walls (28). The presence of vasa vasorum suggests occurrence of hypoxia in the aneurysmal wall as hypoxia induces angiogenesis resulting in sprouting of vasa vasorum across the arterial wall (33). Although similar proportions of vasa vasorum were present in both unruptured and ruptured IA, ultrastructural analysis of these vasa vasorum showed striking difference. Vasa vasorum in ruptured IA exhibited a leaky nature, which seems to act as a gateway for inflammatory cells to enter the IA wall: the endothelial lining of these vasa vasorum had hypertrophic appearance with irregular surface and vacuoles at junctions of adjacent endothelial cells and white blood cells were observed to extravasate into the vessel wall. This results in increased endothelial permeability for circulating lipoproteins, inflammatory cell infiltrates, and red blood cells, and might subsequently lead to further instability of the IA wall.

Thrombus

Although only qualitatively analyzed, presence of thrombus was examined in both ruptured and unruptured aneurysms. In half of the ruptured aneurysms, we observed the presence of fresh and organized thrombus, encompassing predominantly neutrophils and macrophages. The presence of organizing thrombus is considered as a potential risk factor (34) and could also contribute to inflammatory cell infiltration.

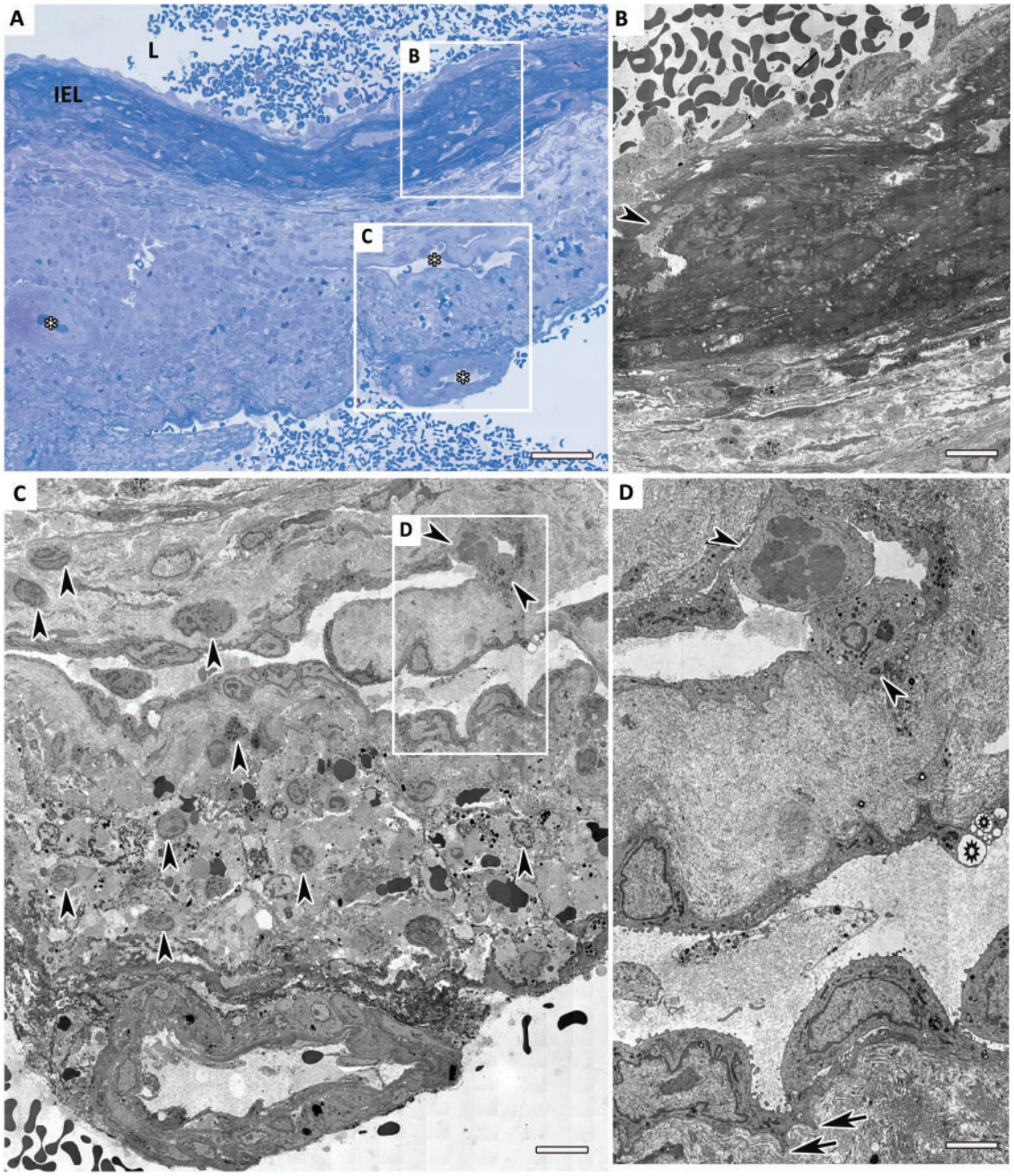

FIGURE 3. Methylene blue-Azur stained light microscopy (LM) and transmission electron microscopy (TEM) images of a ruptured intracranial aneurysm (IA). **(A)** LM image of a ruptured aneurysm wall. Thickened internal elastic lamina (IEL) infiltrated with inflammatory cells. Several large vasa vasorum complexes are present throughout the vessel wall (asterisks). Scale bar = 40 μm. **(B)** TEM image of ruptured IA luminal layer. Presence of a macrophage within the IEL could be seen (white outline). Scale bar = 5 μm. **(C)** Two large vasa vasorum with inflammatory cells within and neighboring regions in the abluminal layer. Scale bar = 5 μm. **(D)** Higher magnification of the "leaky" vasa vasorum shown in Figure 2C. Hypertrophic endothelial cells with irregular surfaces, show pseudopodia-like protrusions (arrows). Vacuoles present at the junction of 2 endothelial cells lining the vasa vasorum (stars). Two inflammatory cells are infiltrating into heavily invaded vessel wall via vasa vasorum (arrowheads). Scale bar = 2 μm.

Taking into consideration that in the current study the time lapsed from the rupture until sample acquisition may have influenced the status of the thrombus and presence of inflammatory cells we cannot conclusively say whether they were formed before or after rupture. In follow up studies, with increased sample size utilizing histology and immunohistochemistry, the role of thrombi in the invasion of inflammatory cells should be addressed.

Foam Cells

One of the most prominent features observed in both unruptured and ruptured IA is the abundance of FC in localized regions within the vessel walls. Quantified regions showed an inverse correlation between FC and macrophages in both groups, indicating the transformation of macrophages into FC, as observed in atherosclerosis (35). It is unlikely that FC presence is associated with risk of rupture since there was no significant difference in the proportions of FC between unruptured and ruptured IA as is also observed in previous studies (11, 15).

Strengths and Limitations

This study included a relatively limited number of 12 patients, but thereby we were able to assess the complete biopsy samples and extensively compare unruptured with ruptured IA both by means of stereology and correlative microscopy. The selection bias is that very small IA, which are entirely included in the clip during microsurgery, could not be included in the study. In addition, there is a large variation of individual IA sizes between ruptured versus unruptured cases studied, thus part of the differences between ruptured and unruptured IA found in our study might relate to size instead of rupture status. Furthermore, clinical risk factors could also play an essential role in remodeling of IA. The number of samples analyzed is insufficient for correlating clinical risk factors to ultrastructural findings. Future research, expanding on the current results, should include larger numbers of patients, using histopathological analysis of the parameters found in the present ultrastructural study in unruptured versus ruptured aneurysmal wall.

Conclusions

Unruptured and ruptured IA have structural differences in internal elastic lamina, vasa vasorum endothelium and inflammatory infiltrates. These results suggest that secondary structural remodeling of the vessel wall (IEL) and infiltration of inflammatory cells via vasa vasorum might be involved in IA rupture. This hypothesis clearly needs further studies and may lead to biomarkers for rupture prone IA by focusing on IEL, vasa vasorum leakiness and the presence of (specific) inflammatory cells. Ideally, management strategies preventing development of vasa vasorum or inflammation to reduce the risk of aneurysmal rupture will be developed based on the results of these studies. Animal studies already showed promising results supporting the use of antiinflammatory treatment strategies in IA as antiinflammatory drugs targeted at suppressing macrophage infiltration were successful in preventing development and/or growth of IA in mice and rats (36, 37).

ACKNOWLEDGEMENT

The authors are grateful to Elly G. van Donselaar and Rob Mesman for expert technical assistance.

REFERENCES

1. Vlak MH, Algra A, Brandenburg R, et al. Prevalence of unruptured intracranial aneurysms, with emphasis on sex, age, comorbidity, country, and time period: A systematic review and meta-analysis. Lancet Neurol 2011;10:626–36
2. Nieuwkamp DJ, Setz LE, Algra A, et al. Changes in case fatality of aneurysmal subarachnoid haemorrhage over time, according to age, sex, and region: A meta-analysis. Lancet Neurol 2009;8:635–42
3. de Rooij NK, Linn FH, van der Plas JA, et al. Incidence of subarachnoid haemorrhage: A systematic review with emphasis on region, age, gender and time trends. J Neurol Neurosurg Psychiatry 2007;78:1365–72
4. Kotowski M, Naggara O, Darsaut TE, et al. Safety and occlusion rates of surgical treatment of unruptured intracranial aneurysms: A systematic review and meta-analysis of the literature from 1990 to 2011. J Neurol Neurosurg Psychiatry 2013;84:42–8
5. Alshekhlee A, Mehta S, Edgell RC, et al. Hospital mortality and complications of electively clipped or coiled unruptured intracranial aneurysm. Stroke 2010;41:1471–6
6. Greving JP, Wermer MJ, Brown RD, et al. Development of the PHASES score for prediction of risk of rupture of intracranial aneurysms: A pooled analysis of six prospective cohort studies. Lancet Neurol 2014;13:59–66.
7. Kataoka K, Taneda M, Asai T, et al. Structural fragility and inflammatory response of ruptured cerebral aneurysms. A comparative study between ruptured and unruptured cerebral aneurysms. Stroke 1999;30:1396–401
8. Scanarini M, Mingrino S, Giordano R, et al. Histological and ultrastructural study of intracranial saccular aneurysmal wall. Acta Neurochir 1978;43:171–82
9. Lang ER, Kidd M. Electron microscopy of human cerebral aneurysms. J Neurosurg 1965;22:554–62
10. Nystroem SH. Development of intracranial aneurysms as revealed by electron microscopy. J Neurosurg 1963;20:329–37
11. Ollikainen E, Tulamo R, Lehti S, et al. Smooth muscle cell foam cell formation, apolipoproteins, and abca1 in intracranial aneurysms: Implications for lipid accumulation as a promoter of aneurysm wall rupture. J Neuropathol Exp Neurol 2016;75:689–99
12. Ollikainen E, Tulamo R, Frösen J, et al. Mast cells, neovascularization, and microhemorrhages are associated with saccular intracranial artery aneurysm wall remodeling. J Neuropathol Exp Neurol 2014;73:855–64
13. Tulamo R, Frösen J, Junnikkala S, et al. Complement activation associates with saccular cerebral artery aneurysm wall degeneration and rupture. Neurosurgery 2006;59:1069–76
14. Frösen J, Piippo A, Paetau A, et al. Remodeling of saccular cerebral artery aneurysm wall is associated with rupture: Histological analysis of 24 unruptured and 42 ruptured cases. Stroke 2004;35:2287–93
15. Frösen J, Tulamo R, Heikura T, et al. Lipid accumulation, lipid oxidation, and low plasma levels of acquired antibodies against oxidized lipids associate with degeneration and rupture of the intracranial aneurysm wall. Acta Neuropathol Commun 2013;1:71
16. Karnovsky M. Formaldehyde-glutaraldehyde fixative of high osmolality for use in electron microscopy. J Cell Biol 1965;27:137–8A
17. Jimenez N, Vocking K, van Donselaar EG, et al. Tannic acid-mediated osmium impregnation after freeze-substitution: A strategy to enhance membrane contrast for electron tomography. J Struct Biol 2009;166:103–6
18. Reid IM. Morphometric methods in veterinary pathology: A review. Vet Pathol 1980;17:522–43
19. Gundersen HJ, Bendtsen TF, Korbo L, et al. Some new, simple and efficient stereological methods and their use in pathological research and diagnosis. Acta Pathol Microbiol Immunol Scand 1988;96:379–94
20. Jones G. The pathohistology of abdominal aortic aneurysm. In: Grundmann R, ed. Diagnosis, screening and treatment of abdominal, thoracoabdominal and thoracic aortic aneurysm. InTech 2011;53–74. doi: 10.5772/746.
21. Humphrey JD, Taylor CA. Intracranial and abdominal aortic aneurysms: similarities, differences, and need for a new class of computational models. Ann Rev Biomed Eng 2008;10:221–46
22. Kojimahara M. Intimal laminated elastosis in the intrarenal arteries. An electron microscopic study. Acta Pathol Japon 1988;38:315–23
23. Krettek A, Sukhova GK, Libby P. Elastogenesis in human arterial disease: a role for macrophages in disordered elastin synthesis. Arterioscler Thromb Vasc Biol 2003;23:582–7
24. Libby P, Ridker PM, Maseri A. Inflammation and atherosclerosis. Circulation 2002;105:1135–43

25. Tulamo R, Frosen J, Hernesniemi J, et al. Inflammatory changes in the aneurysm wall: a review. J Neurointerv Surg 2010;2:120–30
26. Mulligan-Kehoe MJ. The vasa vasorum in diseased and nondiseased arteries. Am J Physiol Heart Circ Physiol 2010;298:H295–305
27. Takaba M, Endo S, Kurimoto M, et al. Vasa vasorum of the intracranial arteries. Acta Neurochir 1998;140:411–6
28. Aydin F. Do human intracranial arteries lack vasa vasorum? A comparative immunohistochemical study of intracranial and systemic arteries. Acta Neuropathol 1998;96:22–8
29. Atkinson JL, Okazaki H, Sundt TM, et al. Intracranial cerebrovascular vasa vasorum associated with atherosclerosis and large thick-walled aneurysms. Surg Neurol 1991;36:365–9
30. Sawyer DM, Pace LA, Pascale CL, et al. Lymphocytes influence intracranial aneurysm formation and rupture: role of extracellular matrix remodeling and phenotypic modulation of vascular smooth muscle cells. J Neuroinflammation 2016;13:185
31. Aoki T, Frösen J, Fukuda M, et al. Prostaglandin E2-EP2-NF-κB signaling in macrophages as a potential therapeutic target for intracranial aneurysms. Sci Signal 2017;10. doi:10.1126/scisignal.aah6037
32. Kleinloog R, van der Vlies P, Deelen P, et al. RNA sequencing analysis of intracranial aneurysm walls reveals involvement of lysosomes and immunoglobulins in rupture. Stroke 2016; 47:1286–93
33. Hickey MM, Simon MC. Regulation of angiogenesis by hypoxia and hypoxia-inducible factors. Curr Top Dev Biol 2006;76:217–57
34. Mehan WA, Romero JM, Hirsch JA, et al. Unruptured intracranial aneurysms conservatively followed with serial CT angiography: Could morphology and growth predict rupture?. J Neurointervent Surg 2014;6: 761–6
35. Jarvilehto M, Tuohimaa P. Vasa vasorum hypoxia: Initiation of atherosclerosis. Med Hypotheses 2009;73:40–1
36. Ikedo T, Minami M, Kataoka H, et al. Dipeptidyl peptidase-4 inhibitor anagliptin prevents intracranial aneurysm growth by suppressing macrophage infiltration and activation. J Am Heart Assoc 2017;6:e004777
37. Shimada K, Furukawa H, Wada K, et al. Protective role of peroxisome proliferator-activated receptor-γ in the development of intracranial aneurysm rupture. Stroke 2015;46:1664–72